Influence of Industrial Lubricant Addition on Heat Transfer Regimes during Spray Cooling

Marija Gajevic Joksimovic*, Ilia V. Roisman, Cameron Tropea, Jeanette Hussong
Institute for Fluid Mechanics and Aerodynamics,
Technical University Darmstadt, Darmstadt, Germany
*Corresponding author: gajevic-joksimovic@sla.tu-darmstadt.de

Abstract
The effect of lubricant additives in distilled water on spray impact onto an extremely hot substrate and the associated heat flux is studied experimentally and modeled theoretically in this study. As a working fluid, mixtures of water with industrial white lubricant in different mixture ratios are used. A high-speed video system is used for the visualization of spray impact and identification of the main hydrodynamic regimes. Measurements of the heat flux during continuous cooling from 445℃ to 100℃ are based on temperature measurements in the substrate at a set of locations, accompanied by the solution of the inverse heat conduction problem. We have discovered that the addition of even small amounts of the lubricant increase significantly the heat flux due to spray cooling, especially at relatively high wall temperatures. The liquid boiling at the substrate leads to an extensive foaming in the near wall region and also to the formation of a deposited layer of the non-volatile components of the mixture. The formation of this layer causes a significant increase of the Leidenfrost point.

Keywords
Lubricant solutions, heat flux regimes, spray cooling.

Introduction

The need for ever higher heat flux removal capacities in various industry fields is best met by spray cooling applications. Among the main advantages of spray cooling technology is the simplicity of the spray generation, possibility of cooling of relatively large surfaces or specific areas of interests. Spray impact onto a hot surface is often used in a variety of industrial applications, such for die forging, hot mill rolling [1] and cooling of power electronics [2]. For some of the mentioned applications, for example during hot die forging, sprays are used not only as a coolant, but also as a transport medium for lubricating liquids.
In [3–6], a comprehensive overview of spray cooling technology with usage of water or another one-component liquid as the working fluid can be found. Spray cooling can produce a significant amount of heat flux, especially when combined with liquid evaporation at temperatures exceeding saturation temperature. However, for surface temperatures that do not exceed the saturation temperature, the cooling is realized mainly through the impact of single drops [7], convection in a thin liquid wall film and through the evaporation at the free surfaces of the liquid layer. At higher substrate wall temperatures, the phenomenon is strongly influenced by nucleate boiling, film boiling or thermal atomization boiling, depending on the substrate temperature, thermal properties of the substrate and liquid, or on impact parameters of the spray.
The addition of surfactants or dissolving of various types of salts in the bulk liquid can greatly alter the phenomenon of boiling; hence, boost spray cooling at higher wall temperatures [8–11]. For example, [12] have noted that the heat flux at the surface of the very hot metal substrates at 900℃, significantly increases by the addition of the dissolved salts in water used for cooling. Behavior and properties of the liquid during spray cooling of hot substrates can change significantly due to the partial liquid evaporation. The concentrations of the less volatile components rise in response. Under some conditions these non-evaporated components deposit on the substrate s a solid layer.

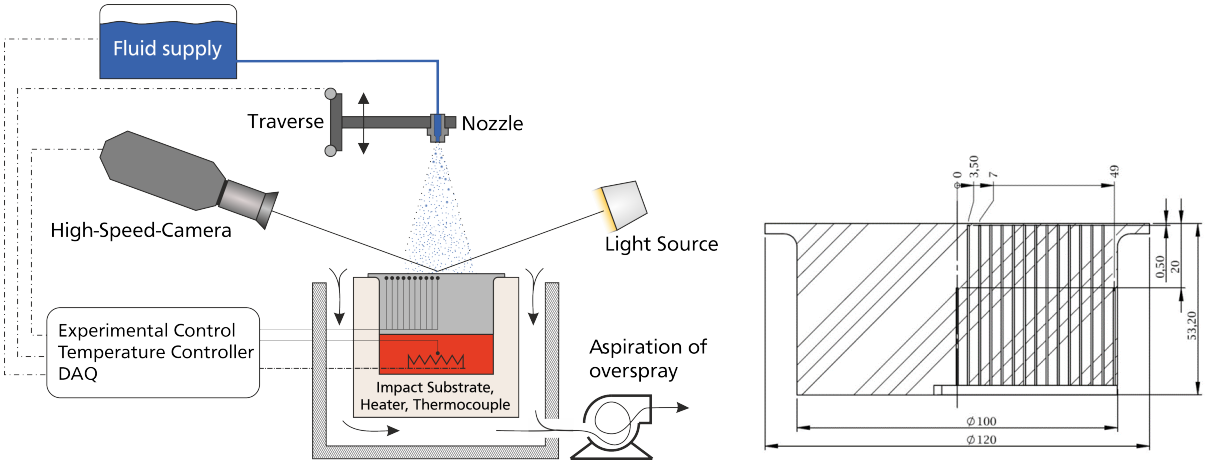

(a) Schematic representation of the spray cooling experimental setup.

(b) Sectional view of the heated target showing the thermocouple positions. Dimensions are in mm.

Figure 1. Experimental setup and the heated target.

The main goal of this investigation is to observe, characterise and analyse the evolution of the heat flux during the spray cooling experiments, using an industrial water/lubricant mixture in different mixture ratios. Focus will be placed on discussing phenomena accompanying different heat transfer regimes during spray impact of a multi-component liquid onto a very hot surface. Temperature and heat flux measurements are performed during continuous cooling of a thick stainless steel target from 445 °C to 100 °C. These measurements are accompanied by high-speed visualizations of an impacting spray at various time instants, allowing identification of different spray cooling hydrodynamic and thermodynamic regimes, as well as the influence of different lubricant concentrations on the latter. It is found that the addition of even small amounts of lubricant significantly increases the heat flux, especially at relatively high wall temperatures. Cooling time is therefore notably reduced in comparison to the pure water case. Moreover, at high temperature spray cooling is accompanied by extensive foaming in the near wall region on substrates. Foaming phenomena and the deposition of the solid layer are associated with a significant increase of the temperature of the Leidenfrost point and almost total suppression of the film boiling regime.

Experimental methodology

Experimental setup

The experimental setup for spray cooling experiments is shown in Fig. 1a. It consists of a spray generation system connected to fluid supply, heated target connected to temperature measurement and control, optical observation system and computer control unit for data acquisition and control of the experimental flow.

A conventional pressure driven, one-component, full-cone atomizer (*Lechler 490.403*) is supplied with water/lubricant mixture, stored in a tank. The atomizer is driven by a gear pump while a flow rate of the fluid passing through the atomiser is measured by a Coriolis mass flow meter (*Optimass 7400 C* from *Krohne*). The atomiser used in our experimental campaign has a bore diameter 1.25 mm, spray angle 45° and operating pressure between 1.5 and 10 bar. The upper limit of operational pressure is, however, dictated by the maximum differential pressure of the gear pump. The spray is characterized using phase Doppler measurements and the mass flow rates. The results of these measurements can be found in [13]. Different impact velocities of the spray droplets are achieved by varying the height of the spray above the hot substrate using a linear traverse. Due to presence of additives, such as surfactants and salts in mixtures used in this experimental campaign, solid residue forms on the substrate once each spray experi-

ment is completed. Therefore, the substrate surface must be cleaned after each experiment. A reservoir containing a mixture of water and isopropanol is connected to a fluid supply line with valves for this purpose. The valves downstream of the fluid tank are closed during the cleaning, in order to supply only the cleaning liquid to the entire system.
The heated target is a circular cylinder top end (diameter 100 mm and height 53.2 mm) which is carefully thermally sealed. The target is heated by a four cartridge heaters *hotset hotrod HHP*, placed in a copper disc that is fastened to the cylinder bottom. Total power of the all heaters is 2 kW. To presume that heat transfer occurs solely through the top surface of the heated target, the target sides and bottom are insulated. Material of the target is stainless steel, with mirror polished upper surface. Polishing was achieved through lapping and polishing processes, resulting in average roughness of polished surface < 0.03 μm. It was shown that stainless steel exhibits good resistance against corrosion and oxidation, thus, the spray target used in this experimental campaign endured more than 200 cooling experiments. The setup is designed for surface temperatures up to 500℃.
The observation system consists of a CMOS high-speed camera equipped with two different lenses and a back light illumination source. A camera *Vision Research Phantom v2012*, which can achieve a maximum resolution of 1280$\times$800 pixels at 55000 fps, is used to record side-view images and videos of the spray impact. The high-speed camera is additionally equipped with a *Tamron* 180 mm macro optical lens. The back light illumination consists of a high powered light source (LED Illumination) and a diffusor plate.

Measurement technique for heat flux and surface temperature

The temperature readings are acquired from thermocouples embedded inside the target. In Fig. 1b the position of the thermocouples is shown. The thermocouples are type K, class 1, with 0.5 mm shield diameter. The measuring tip is open and aligned with the shield. This configuration ensures a fast response time. Thermocouple placement was arranged in two rows. The first row is located 0.5 mm below the surface to achieve a quick response time of all thermocouples. The radial distance between each sensor in the first row is 3.5 mm to account for any radial distribution of the heat flux. The second row is 20 mm below the surface to make the inverse heat conduction procedure (IHCP) independent of the boundary condition at the bottom of the target. The thermocouples are bonded inside holes of 0.6 mm in diameter using a thermally high conductive adhesive (*Aremco Ceramabond 569 VFG*). Temperatures are sampled at a sample rate of 95 Hz using *National Instruments NI 9212* thermocouple input modules attached to a *National Instruments cRio 9074*. Heat flux problem is assumed to be two-dimensional, axisymmetric and having adiabatic boundary conditions at the curved surface area. The housing with the heated target on top was completely insulated on all sides except the spray surface. The solution of inverse heat conduction problem [14] allows to estimate the temperature and heat flux at the substrate interface.

Preparation of lubricant solutions

The industrial lubricant LUBRODAL F327,* produced by company Fuchs LUBRITECH, is used as a base for the preparation of the solutions used in experimental campaign. The lubricant LUBRODAL F327 represents a water-miscible, graphite free, die lubricant with excellent separation effects for hot and warm forging of steel. It is widely used for different forging operations in industry because of quick formation of a well visible and touch-resistant lubrication film after spraying to the hot tool surfaces.
Lubricant is supplied as a concentrate, containing a specific amount of organic salts that provide lubrication when utilized. Organic and inorganic components (surfactants and binders) are present in the concentrate as well, in order to stabilize it and promote the spreading and formation of adherent lubricant layers on the die surface. Prior to lubricant usage in spray system,diluting with water in desired ratio is necessary. Further stirring of the working mix-

*https://www.fuchs.com/lubritech/en/product/product/144158-lubrodal-f-327

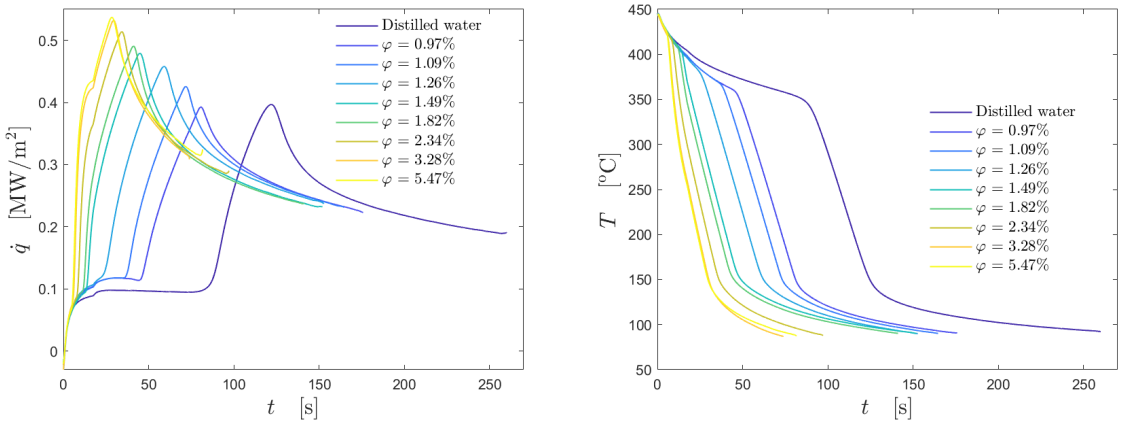

(a) Temporal evolution of the heat flux for different volume concentrations.

(b) Temperature evolution for different volume concentrations.

Figure 2. Temperature and heat flux evolution during spray cooling of a thick target for different volume concentrations of lubricants.

ture is not necessary, because the main component, organic salt, is completely dissolved in water. Solutions of different salt volume concentrations are prepared by mixing the concentrate with distilled water. In this study the volumetric concentrations of the solutions range from $\varphi = 0.97\,\%$ to $\varphi = 5.47\,\%$.
The boiling temperature of the mixture is $T_{\mathrm{sat}} = 100°$C. The surface tension of the different solutions has been measured with a tensiometer. The surface tension of the solutions is respectively: $\sigma = 58.95$ mN/m for $\varphi = 5.47\,\%$, $\sigma = 61.63$ mN/m for $\varphi = 2.34\,\%$ and $\sigma = 64.28$ mN/m for $\varphi = 1.49\,\%$.

Results and discussion

In all experiments, target is first heated to a uniform initial temperature. The inception of the spray impact onto the target is synchronized with the switching off the target heating. The spray parameters used in this experimental campaign are: mass flow $\dot{m} = 62.1$ kg/h (dense spray), mean drop diameter $D_{10} = 78.7\,\mu$m and mean impact velocity $U = 14.05$ m/s. After each experiment (and complete liquid evaporation), solid residue on the substrate is carefully removed prior to the next experiment.

Evolution of the heat flux and the wall temperature during spray cooling

The time evolution of the surface temperature and of the heat flux is shown in Fig. 2. The initial wall temperature is 445 °C. The experiments were stopped when the first thermocouple reading reached 100 °C. Although the slopes of the curves in Fig. 2(a) are similar, especially in the nucleate boiling regime, they differ significantly at high temperatures between the start of the cooling experiments and the Leidenfrost point. For distilled water, at the very high temperature, the film boiling regime is observed for approximately 80 seconds, where the substrate is covered by a thin vapor layer. Local heat flux in this period can be described as low and remaining nearly constant until the temperature of Leidenfrost point is reached. The heat flux at this temperature reaches a minimum. Almost immediately afterwards, the slope of the curve changes abruptly, caused by the appearance of liquid patches on the substrate. This phenomenon is associated with the transitional boiling regime. Next, an increase of the liquid patches progresses rapidly, thus increasing the value of heat flux and consequently reaching its maximum at the CHF point. After reaching the critical heat flux point, a completely wetted surface is present, identifying the nucleate boiling regime where the slope of the curve falls to a lower plateau. The end of the cooling process is estimated to be approximately 260 seconds.

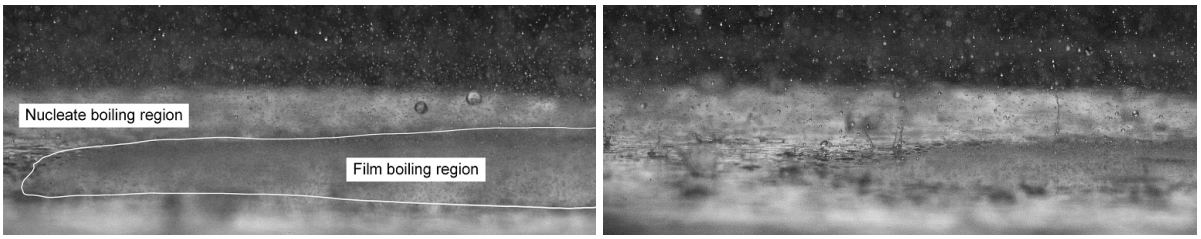

(a) Dominance of a film boiling region.

(b) Expansion of the nucleate boiling region.

(c) Vanishing of the film boiling region.

(d) Wetted substrate.

Figure 3. Distilled water spray impact. Regions of different thermodynamic regimes at the substrate. Spray parameters correspond to the case shown in Fig.2(a)-(b) for distilled water. Initial wall temperature was $T_{\mathrm{w0}} = 445$ ℃.

On the other hand, even with small amount of lubricant added to a spray liquid, the entire process is changed substantially. The lowest volumetric concentration used (lowest lubricant concentration) corresponds to $\varphi = 0.97\,\%$. In this case, as it can be seen in Fig. 2, the critical heat flux remains at the same order of magnitude as that for water, but the duration of the cooling process decreases. The Leidenfrost point is found to be at a higher temperature than that for pure water, thus significantly decreasing the duration of the film boiling regime. Different temperatures identified as Leidenfrost points for different solutions can be better observed from Fig. 2(b). Namely, the Leidenfrost point seems to be nearly independent of the spray properties. Instead, it is strongly influenced by the material of the substrate and fluid: for a very high volumetric concentration ($\varphi = 5.47\,\%$), the film boiling phenomenon is almost totally suppressed even at a Leidenfrost point at a very high temperature, approximately 420℃. With a decrease in volumetric concentration of lubricant solutions, the Leidenfrost point is accordingly moved to a lower temperatures. However, the duration of film boiling regime is still considerably smaller than that for distilled water case.

Phenomena of spray impact onto a hot substrate

Typical phenomena observed during spray cooling of a thick metal target by distilled water [15] are shown in Fig. 3 with mentioned heat transfer regimes, present in different regions. In Fig. 3 (a) presence of a "darker" region corresponds to a film boiling region where drop rebound is dominant due to a very high temperature of a metal target. Outside of the film boiling region, presence of liquid film can be observed, thus identifying nucleate boiling region, with apparently completely wetted area. Therefore, initially the film boiling region corresponds to the heating region of the target. The cooling can be described as non-uniform since the metal target is cooled not only by the spray impacting on the center of the target, but also by the liquid film outside. This explains reduction of a film boiling region, emergence of the wetted spots and at the end, completely developed liquid film on the substrate surface, as seen in Fig. 3(d). This result shows that the spray cooling phenomenon is a three-dimensional phenomenon even if the thermal boundary layer is much thinner than the thickness of the substrate.

When a small amount of liquid lubricant is added to the liquid, the observed phenomena change significantly. An example is shown in Fig. 4. Separate wet spots form on the substrate surface within a short time after spraying begins. This behavior is observed on a very high temperature, resulting in perforation of a vapor layer formed on a substrate. Next, liquid volumes generate a foam on a very hot substrate, thus reducing the duration of film boiling regime. The foam region

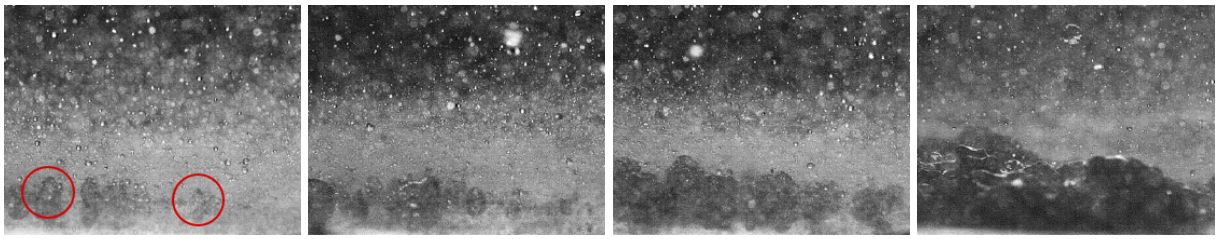

Figure 4. Impact of the $\varphi = 2.34\,\%$ solution. Shadowgraph visualisations of a foaming phenomenon in 4 stages: from first appearance of foaming bubbles (denoted with red circles) to a completely developed foaming layer. Spray parameters correspond to the case shown in Fig.2(a)-(b). Initial wall temperature was $T_{w0} = 445$ ℃.

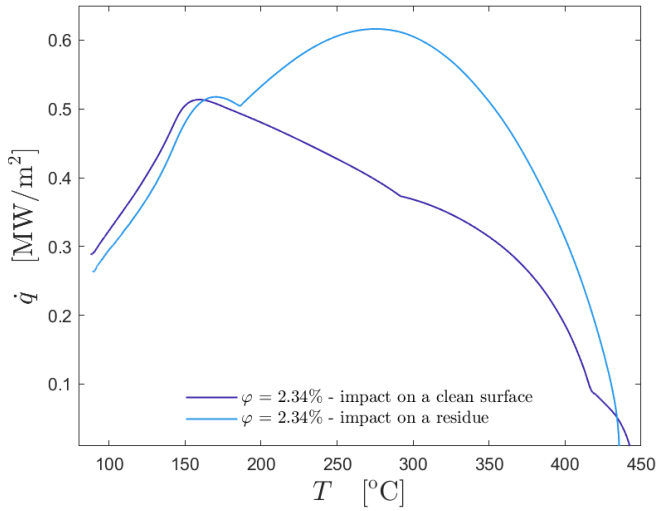

Figure 5. Evolution of a heat flux in dependence from substrate temperature for impact on a clean surface and impact on a residue. In both cases, solution $\varphi = 2.34\,\%$ is used.

expands until it forms a fully developed, relatively thick foam layer which coats the surface exposed to spray. Appearance of a foam accelerates the whole cooling process, resulting in shorter cooling times, identified only with usage of lubricant solutions.

Suppression of film boiling at high wall temperatures

At the substrate temperatures exceeding the Leidenfrost point, an extensive liquid evaporation leads to the formation of a thin expanding vapor layer. For one-component liquids, like distilled water, the vapor layer prevents the substrate wetting, thus leading to the drop rebound.

Addition of small quantities of lubricants leads to the significant change of the hydrodynamic regime of drop and spray impact caused by the suppression of the film boiling phenomenon. This suppression has been recently observed for suspensions [16] and for the lubricant solutions containing salts. The suppression of the film boiling phenomenon in all these cases is accompanied by the formation of a solid layer of non-volatile components of the mixture deposited on the substrate. This layer is wettable even at very high temperatures. Mentioned accreted layer leads to the pinning of the impacting drop, preventing drop rebound. Similar phenomena has been observed on porous nano-fiber coatings [17].

Figure 5 depicts difference between the spray impact on a clean, polished, surface and on the other hand, spray impact on a already formed residue from the last experiment for solution $\varphi = 2.34\,\%$. The difference is shown by means of the heat flux evolution in dependence of surface temperature during the cooling process. When residue is already present, the presence of film boiling regime cannot be observed. Namely, shortly after the spray starts, solid residue deposited on a substrate generates a dense foam layer in contact with incoming spray liquid, thus preventing drop rebound. Accordingly, the slope of the corresponding curve on Fig. 5

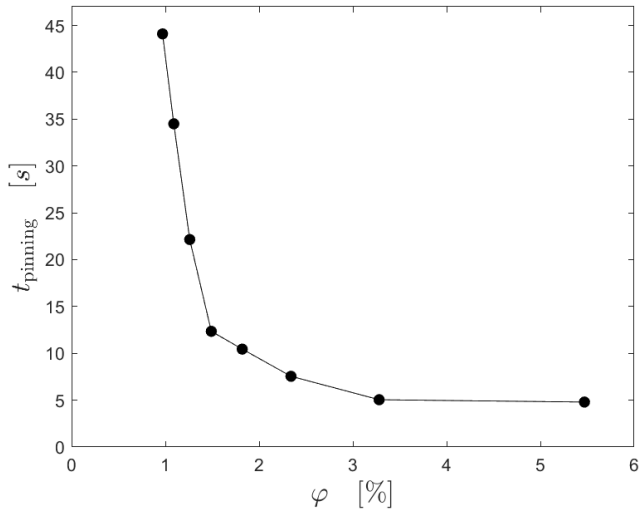

Figure 6. Dependence of the pinning time t_{pinning} on solution concentration φ.

increases significantly, signifying higher heat flux and a better cooling rate. In this case, the foam layer is discontinued when the temperature reaches 190 ℃, pointing to the inception of apparently completely wetted surface which corresponds to the nucleate boiling regime. The suppression of the film boiling regime is caused therefore by the pinning of the contact line, which prevents the drop rebound.

For spray impact of a lubricant solution on a heated target, one can estimate a pinning time t_{pinning} which is characterized by an inception of a sharp reduction of the substrate temperature caused by a fast increase of heat flux. These temperatures can be determined from the data shown in Fig. 2. The dependence of t_{pinning} on the lubricant concentration is shown in Fig. 6. The operating parameters of spray cooling experiments are the same as in Fig. 2. The pinning time reduces for larger concentrations since the presence of the dissolved salt increases the rate of the formation of deposited layer.

Conclusions

In this study, the spray impact of different lubricant solutions onto a very hot substrate has been studied. The effective material properties the solutions are very similar and rather close to that of distilled water. Nevertheless, the presence of the dissolved organic salts in the spraying liquid influences significantly the heat transfer regimes during the spray cooling process.

If the initial substrate temperature is high enough, higher than the Leidenfrost point, spray impact is accompanied by film boiling of each impacting drop of a distilled water spray. During film boiling, drop rebound from the solid substrate is observed. The heat flux is relatively low due to the insulating properties of the vapor layer.

However, the hydrodynamic behaviour of lubricant solutions at the same temperatures is completely different. Spray impact leads to a fast formation of a thick foaming layer, whose thickness is larger than the initial diameter of the primary drops in the spray. Moreover, liquid evaporation due to a spray impact leads to the formation of a wettable deposited layer of the less-volatile components in the mixture. The drop contact line is pinned at the deposited layer. Therefore, the drop rebound is prevented and the film boiling regime is suppressed for lubricant solutions. In this range of temperatures heat transfer caused by spray cooling by lubricant solutions is much higher than that during spraying of distilled water.

Nomenclature

t time [s]

t_{pinning} pinning time [s]

φ	volume concentration [%]
$\dot{m}$	spray mass flow [kg/h]
σ	surface tension [N/m]
D_{10}	mean drop diameter [m]
U	mean droplet velocity [m/s]
T_{w0}	initial wall temperature [°C]
T	surface temperature [°C]
$\dot{q}$	local heat flux [W/m^2]

Acknowledgements
The authors gratefully acknowledge financial support from the Deutsche Forschungsgemeinschaft (DFG) in the framework of SFB-TRR 75 (TP T02, project number 84292822).

References

[1] Chen, S.-J., Tseng, A. A., 1992, *International Journal of Heat and Fluid Flow*, 13 (4) pp. 358–369.
[2] Chen, H., Ruan, X.-h., Peng, Y.-h., Wang, Y.-l., Yu, C.-k., 2022, *Sustainable Energy Technologies and Assessments*, 52 p. 102181.
[3] Kim, J., 2007, *International Journal of Heat and Fluid Flow*, 28 (4) pp. 753–767.
[4] Liang, G., Mudawar, I., 2017, *International Journal of Heat and Mass Transfer*, 115 pp. 1174–1205.
[5] Liang, G., Mudawar, I., 2017, *International Journal of Heat and Mass Transfer*, 115 pp. 1206–1222.
[6] Breitenbach, J., Roisman, I. V., Tropea, C., 2018, *Experiments in Fluids*, 59 pp. 1–21.
[7] Yarin, A. L., Roisman, I. V., Tropea, C., 2017, Collision phenomena in liquids and solids, Cambridge University Press, Cambridge, UK.
[8] Qiao, Y. M., Chandra, S., 1998, *Journal of Heat Transfer*, 120 (1) pp. 92–98.
[9] Ravikumar, S. V., Jha, J. M., Sarkar, I., Pal, S. K., Chakraborty, S., 2014, *Applied thermal engineering*, 64 (1-2) pp. 64–75.
[10] Abdalrahman, K. H. M., Sabariman, Specht, E., 2014, *International Journal of Heat and Mass Transfer*, 78 pp. 76–83.
[11] Pati, A. R., Behera, A., Munshi, B., Mohapatra, S. S., 2017, *Experimental Thermal and Fluid Science*, 89 pp. 19–40.
[12] Mohapatra, S. S., Ravikumar, S. V., Jha, J. M., Singh, A. K., Bhattacharya, C., Pal, S. K., Chakraborty, S., 2014, *Heat and Mass Transfer*, 50 (5) pp. 587–601.
[13] Tenzer, F. M., 2020, Heat transfer during transient spray cooling: An experimental and analytical study, Phd thesis, Technische Universität Darmstadt, Darmstadt, Germany.
[14] Monde, M., Arima, H., Liu, W., Mitutake, Y., Hammad, J., 2003, *International Journal of Heat and Mass Transfer*, 46 pp. 2135–2148.
[15] Tenzer, F., Roisman, I. V., Tropea, C., 2019, *Journal of Fluid Mechanics*, 881 pp. 84–103.
[16] Gajevic Joksimovic, M., Schmidt, J. B., Roisman, I. V., Tropea, C., Hussong, J., 2022, *Soft Matter*, submitted.
[17] Weickgenannt, C. M., Zhang, Y., Sinha-Ray, S., Roisman, I. V., Gambaryan-Roisman, T., Tropea, C., Yarin, A. L., 2011, *Physical Review E*, 84 (3) p. 036310.